# The Zeeman Effect

James Amarel and Kevin Pederson

March 17, 2017

## 1 Goal

To measure the Bohr magneton by determining the splitting of the electronic energy levels through application of a magnetic field to a sample of excited Cadmium atoms.

## 2 Introduction/Background

It is a common occurrence for the energy levels of a system to depend in some way upon its angular momentum, and yet in the case of a free Hydrogen atom, it isn't until one accounts for the effects of special relativity that the degeneracy in the principle quantum number is broken. With the introduction of intrinsic angular momentum, the nucleon and electron constituents of atoms will couple to the magnetic field created by the relative motion of their charged neighbors and to any external magnetic influence in such a way that each spinned particle feels a torque tending to align its magnetic moment with the direction of the field. For a single orbiting electron, the introduction of an external magnetic field translates to the perturbation Hamiltonian

$$H' = -(\mu_L + \mu_S) \cdot \vec{B}_{Ext} = \frac{e}{2m}(\vec{L} + 2\vec{S}) \cdot \vec{B}_{Ext} \tag{1}$$

where, across the second equality, the orbital dipole moment, $\mu_L$, and the magnetic dipole moment, $\mu_S$, have been cast in terms of the angular momentum operator, $\vec{L}$, and the spin operator, $\vec{S}$, respectively [1]. In the proceeding experiment we apply a magnetic field of order 0.2 T to a Cadmium lamp in

order to observe the splitting of the electronic energy levels and analyze the results through weak-field Zeeman effect theory, as our applied field should be considerably weaker than the internal magnetic field strength, which is on the order of 0.3 T for Hydrogen and likely greater for Cadmium [2]. Perturbation theory predicts an energy shift as follows

$$\Delta E = \langle H' \rangle = \mu_B g_j B_{Ext} m_j \tag{2}$$

where $\mu_B = \frac{e\hbar}{2m} = 5.788 \times 10^{-5}$ eV/T is called the Bohr magneton, $g_j$ is the so-called Lande g-factor,

$$g_j = \Big[1 + \frac{j(j+1) - l(l+1) + s(s+1)}{2j(j+1)}\Big] \tag{3}$$

and $m_j$ is the magnetic quantum number.

The above analysis can be applied to composite systems through the introduction of total quantum numbers, where the system state is represented by the spectroscopic notation of $^{2S+1}L_J$. Cadmium has two valence electrons outside its filled 4d shell and when excited will emit photons to make transitions from level 5s6d ($^1D_2$) to level 5s6p ($^1P_1$), both of which are spin zero singlets that satisfy the selection rule $\Delta m_j = 0, \pm 1$. In this case, $g_j$ collapses to unity and Equation 2 reduces to $\Delta E = \mu_B B_{Ext} m_j$. A schematic of these transitions is seen in Figure 1; note that even though we have gone from one decay path to nine, there are only three uniquely emitted photon wavelengths because of selection rule $\Delta l = \pm 1$ and due to the fact that the split from the $m_j = 0$ line by the $m_j = \pm 1, \pm 2$ lines is equivalent in magnitude for both $^1D_2$ and $^1P_1$. Therefore, it is possible to measure $\mu_B$ by applying a known magnetic field and recording the energy of the emitted photons.

# 3 Procedures and Data

In order to measure the Bohr magneton, we used the apparatus outlined in Figure 2 to subject a source of excited Cadmium to an external magnetic field, which is generated by running a current through two coils of wire placed adjacent to the Cadmium lamp on separate sides.

A portion of the transition emitted light travels through a series of optical instruments, of which a schematic is shown in Figure 3, where parallel rays exit a condensing lens after first passing through a color filter that is chosen to match the 643.8 nm line of the unshifted transition from $^1D_2$ to

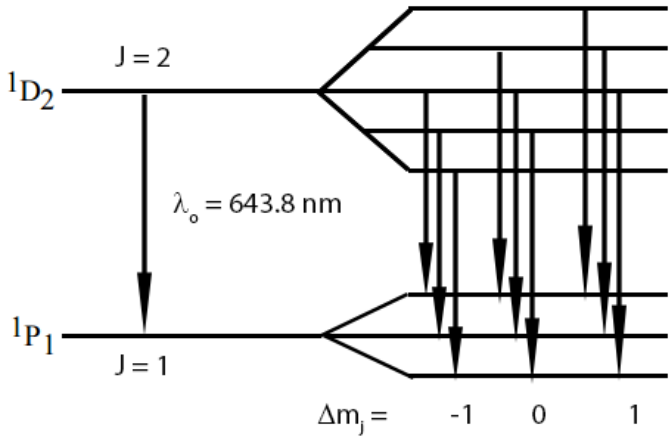


Figure 1: Transition scheme and splitting for Cadmium in the Zeeman effect.

$^1P_1$. A polarizer is added as the next element to take advantage of the fact that photons emitted via the Zeeman effect are polarized according to the magnetic field direction [3]. In the case of $\Delta m_j = 0$, light is polarized parallel to the direction of the applied field, and for $\Delta m_j = \pm 1$, light is polarized perpendicular relative to $\vec{B}$, which allowed us remove the $\Delta m_j = 0$ line - so that we could easily distinguish the $\Delta m_j = \pm 1$ peaks - by setting to polarizer to disallow the transmission of parallel polarized light.

With applied field $B \approx 0.3$ T, the expected Zeeman shift is on the order of $10^9$ Hz, necessitating the use of high resolution spectroscopy and the reason for our choice to include a Fabry-Perot interferometer as the next optical element. The interferometer consists of two highly reflective surfaces aligned parallel to each other, separated by a glass medium of thickness $t \approx 1$ cm, and tuned such that incident rays from the Cadmium source form standing waves between the plates, which is the condition required for transmission [3]. Off resonance wavelengths are reflected immediately and, consequently, do not travel towards the camera. This mechanism allows for high resolution measurements because its output, as viewed from an eyepiece past the final focusing lens, is a series of coaxial rings that gain sharpness from the large number of multiply reflected rays constructively interfering at the same point. When two rays of slightly different wavelength, and still near resonance, enter the interferometer, they will each form their own distinct ring pattern with an angular ring separation that is related to the difference in wavelengths.

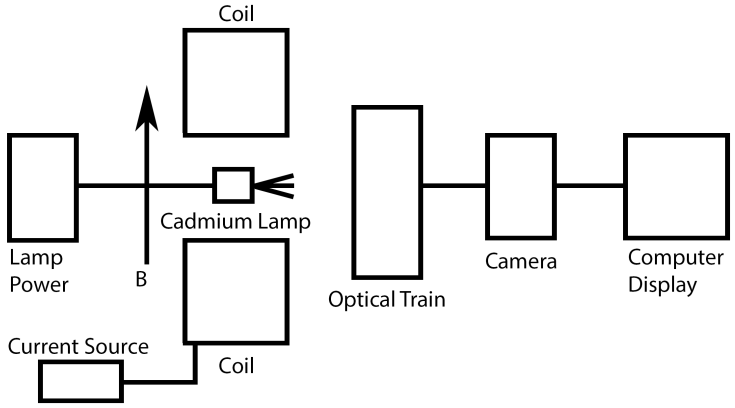


Figure 2: Block diagram of the experimental apparatus. A Cadmium lamp is placed between two magnetic field generating coils, which emits photons that are captured by the optical train and fed through a camera that is linked to intensity analysis software.

After aligning the optics so that a clear and distinct ring pattern was visible through an eyepiece, we used a Gauss meter to measure the resulting magnetic field at the location of the Cadmium lamp for various choices of current through the pair of coiled wires, which we used in Figure 4 to determine a quartic fit for the magnetic field as a function of applied current.

Then, we replaced the eyepiece lens with a CCD camera which connected via USB to a computer software and reported the image intensity according to the deviation angle from the camera center. The camera was aligned to situate the middle sensor in the center of the Fabry-Perot ring by translation and height adjustments until the two peaks corresponding to the smallest ring were maximally tall and sharp. Additionally, we used a feature within the analysis software to set the $0^o$ origin in the center of the two largest peaks.

Next, and with the field off, we selected the largest of these two peaks and marked its angular position. Then, we rotated the polaroid to extinguish the $\pi$ light and began to incrementally increase the applied field. At each field value we recorded the applied current and the angular positions of both shifted peaks, which is seen in Table 1.

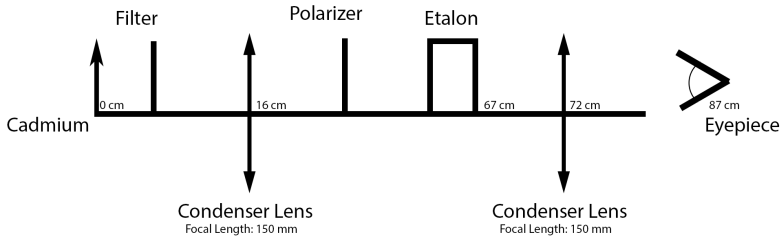


Figure 3: Schematic of the optical train. The Cadmium emission travels through a 644 nm filter and is focused to infinity by a positive lens of focal length 150 mm. The rays then pass through a polarizer, a Fabry-Perot interferometer, and finally are focused to the eyepiece by another lengths of focal length 150 mm.

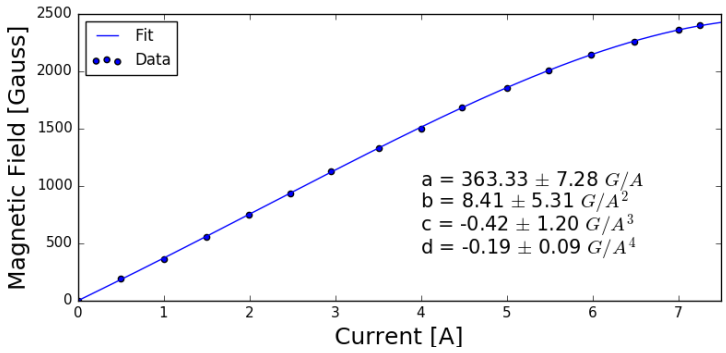


Figure 4: Measured magnetic field at the Cadmium location as a function of the applied current and the results of a quartic polynomial fit, $B = aI + bI^2 + cI^3 + dI^4$, to the data. Where $B$ is the resulting magnetic field, $I$ is the applied current, and $a, b, c, d$ are the fit parameters.

# 4 Analysis and Discussion

Light incident upon the camera array was recorded at some angle, call it $\alpha$, after refracting out through the interferometer according to Snell's law

$$sin(\alpha) = nsin(\beta) \tag{4}$$

where $n = 1.46$ is the index of refraction between the reflective plates, and $\beta$ is the refraction angle of light entering the interferometer. The optical path

Table 1: Angular positions of the left and right shifted peaks according to the applied magnetic field. Here the central, unshifted, peak lay at $0.770^o$. Uncertainty in angular measurements is estimated to be $0.0025^o$, in accordance with the software interval spacing of $0.005^o$.

| Current [A] | $\sigma_-$ [Deg] | $\sigma_+$ [Deg] | Field [G] |
|---|---|---|---|
| 3.39 | 0.722 | 0.818 | 1290 |
| 3.98 | 0.711 | 0.828 | 1500 |
| 4.41 | 0.706 | 0.839 | 1660 |
| 4.81 | 0.7 | 0.845 | 1800 |
| 5.29 | 0.695 | 0.85 | 1950 |
| 5.87 | 0.684 | 0.861 | 2110 |
| 6.35 | 0.684 | 0.871 | 2230 |
| 6.87 | 0.679 | 0.877 | 2340 |

difference for one set of reflections within the interferometer is $\delta = 2nt\ cos(\beta)$, where t is mirror separation, requires the following condition for constructive interference

$$m\lambda = 2nt\ cos(\beta) \tag{5}$$

where $m$ is some integer assuring that the path differences is an integral number of the wavelength, $\lambda$. Then by considering two nearly equivalent wavelengths, $\lambda_1$ and $\lambda_2$, we can write

$$\frac{\lambda_2 - \lambda_1}{\lambda_1} = \frac{\Delta\lambda}{\lambda} = \frac{cos(\beta_2)}{cos(\beta_1)} - 1 \tag{6}$$

where $\beta_1$ and $\beta_2$ are the refraction angles corresponding to $\lambda_1$ and $\lambda_2$, respectively. A small change in the photon energy, $E = hc/\lambda$, with wavelength is equivalently

$$\delta E = \frac{\partial E}{\partial \lambda}\Delta\lambda = -\frac{hc}{\lambda}\frac{\Delta\lambda}{\lambda} \tag{7}$$

where $\frac{\Delta\lambda}{\lambda}$ is determined from Equation 6, $h$ is Planck's constant, and $c$ is the speed of light.

Each angle in Table 1 can be used with Equation 4 to find the corresponding value for $\beta_2$, where $\beta_1$ is determined by the undeflected line, and used in conjunction with Equation 6 and Equation 7 to determine the change in

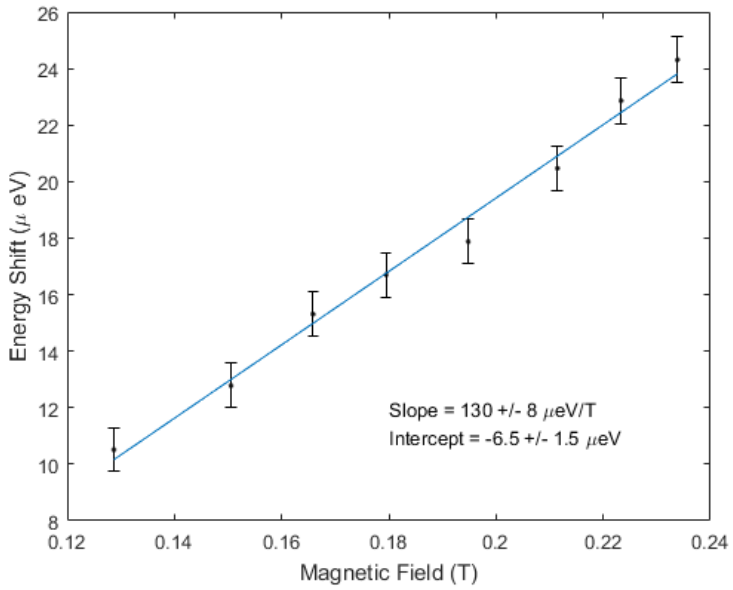


Figure 5: Measured relationship between $\Delta E$ and the applied magnetic field, where the slope of the fitted line should be the value for $\mu_B$. The fit and uncertainty is estimated using the standard least-squares fitting seen in Taylor's error analysis text [4].

energy associated with the shifted level. In Figure 5, we plot the $\Delta E$ for each value of $\sigma_+$ against the magnetic field used to produce that shift. According to Equation 2, the slope of this line should be $\mu_B = 57.88$ $\mu$eV/T, but our measured value of $\mu_B = 130 \pm 8$ $\mu$eV/T is quite far off. We expect there must have been an issue in data collection, as this result is far greater than the accepted value and the uncertainty is too small to contain the accepted value.

We note that the angular splitting is reasonably symmetric about the unshifted peak, so issues with the angle of the camera can be ruled out. It is possible that the middle of the camera array was not in the center of the ring pattern, which could have caused the lines appear to shift further than the true amount. We found the same issue for six data sets, some of which were taken on separate days. Additionally, there were problems with reproducing the data upon returning to a weaker magnetic field from a strong one. We attempted to adjust for this by remeasuring the magnetic field under the

assumption that the coils had grown too warm, but this does not seem to be the issue because it did not have a meaningful effect on the calculations.

# 5 Conclusion

At some point during the procedure, we errored in such a way that we were unable to measure a believable value for the Bohr magneton. We found $\mu_B = 130 \pm 8$ $\mu$eV/T, when instead it should have been on the order of $\mu_B = 57.88$ $\mu$eV/T. Currently, the reason for this poor measurement is unknown, as we are certain that we observed splitting of the energy levels due to the Zeeman Effect. When viewing the sample through an eyepiece there was a clear ring pattern that split into three when the magnetic field was applied and we verified these observations on the computer display, which showed a number of well defined peaks that tapered off in intensity as they grew farther from the center.

# References


[1] David J Griffiths. *Introduction to Quantum Mechanics*. Pearson, 2005.

[2] Randy Harris. *Modern Physics*. Pearson, 1998.

[3] Adrian C. Melissinos. *Experiments in Modern Physics*. Academic Press, 2003.

[4] John R. Taylor. *An Introduction to Error Analysis*. University Science Books, 1997.